

this latter presentation following sclerotomal distribution. Long bones of the lower limbs are most frequently affected<sup>(1-5)</sup>. The disease rarely affects the spine, skull and the face. The diagnosis is essentially clinical and radiological. Laboratory tests results are usually normal and histological findings are nonspecific.

The classical radiological presentation is that of sclerosis in only one side of the cortical bone, with linear and segmental distribution, resembling melted candle wax dropping along the bone axis and projecting over the medullary space. Such an alteration may distally extend to finger bones.

Other observed presentations are similar to osteoma, striated osteopathy, osteopoikilosis, and myositis ossificans, with calcifications in adjacent soft tissues<sup>(1)</sup>.

Computed tomography (CT) shows in more detail the sclerotic alterations as well as reduction of the medullary space. At magnetic resonance imaging (MRI) such alterations present with low signal intensity at T1- and T2-weighted sequences, a finding that is compatible with cortical bone. The involvement of soft tissues may also be observed, with variable calcification degrees at CT; and MRI shows images with heterogeneous signal intensities corresponding to mineralization, areas of fat and fibrovascular tissue<sup>(1,2)</sup>.

Thus, melorheostosis is highlighted as a relevant differential diagnosis among bone diseases, particularly because of the characteristic radiographic findings of this disease.

#### REFERENCES

1. Suresh S, Muthukumar T, Saifuddin A. Classical and unusual imaging appearances of melorheostosis. *Clin Radiol*. 2010;65:593–600.
2. Nuño C, Heili S, Alonso J, et al. Melorheostosis: presentación de un caso y revisión de la literatura. *Rev Esp Enferm Metab Oseas*. 2001;10:50–5.
3. Salman Monte TC, Rotés Sala D, Blanch Rubió J, et al. Melorheostosis, a case report. *Reumatol Clin*. 2011;7:346–8.
4. Mariaud-Schmidt RP, Bitar WE, Pérez-Lamero F, et al. Melorheostosis: unusual presentation in a girl. *Clin Imaging*. 2002;26:58–62.
5. Gagliardi GG, Mahan KT. Melorheostosis: a literature review and case report with surgical considerations. *J Foot Ankle Surg*. 2010;49:80–5.

Paulo Marcus Vianna Franca<sup>1</sup>, Cid Sérgio Ferreira<sup>1</sup>,  
Reginaldo Figueiredo<sup>1</sup>, João Paulo Kawaoka Matushita<sup>1</sup>

1. Universidade Federal de Minas Gerais (UFMG), Belo Horizonte, MG, Brasil. Mailing Address: Dr. Paulo Marcus Vianna Franca. Rua Itai, 570, ap. 102, Santa Efigênia. Belo Horizonte, MG, Brazil, 30260-290. E-mail: pmviannafranca@gmail.com.

<http://dx.doi.org/10.1590/0100-3984.2013.0019>

#### Pre- and postnatal findings of a *dicephalus tetrabrachius-dipus* conjoined twins with a diaphragmatic hernia

Dear Editor,

A 17-year-old primigravida attended the service at the 31st gestational week for evaluation of monochorionic, monoamniotic twin gestation. First trimester sonographic images were not available. Morphological ultrasonography (US) demonstrated the fetuses joined at the level of their abdomen and pelvis, and presence of a diaphragmatic hernia in the second twin. The woman denied previous history of health problems or use of medicines and illicit drugs. Her 25-year-old husband was healthy, with negative history of consanguinity. No family history of genetic diseases and malformations was reported. Fetal magnetic resonance imaging (MRI) revealed a *dicephalus tetrabrachius-dipus* conjoined twin. The fetus at right presented with a left diaphragmatic hernia containing stomach, small bowel and colon. The twins shared a single liver and a urinary bladder. Two kidneys connected each other at the level of their lower poles, and two vertebral spines were fused at the level of the sacrum (Figure 1). Echocardiography was normal.

The conjoined twin was born by Cesarean section at the 35th gestational week, weighting 3,765 grams. Upper eyelid coloboma was found in the twin with diaphragmatic hernia. Radiographic evaluation demonstrated vertebral spines fusion at the level of the lumbar region, besides the presence of bowel loops in the thoracic cavity of the twin at right (Figure 2). Surgery for the diaphragmatic hernia could not be performed. The conjoined twin died at the 17th day of life.

Imperfect twinning occurs in approximately one per 250,000 live births<sup>(1,2)</sup> and is classified according to the fusion site added by the term *pagus*<sup>(3)</sup>. “Parapagus” twins (meaning “extensive lateral fusion”) correspond to 28% of cases of conjoined twins<sup>(4)</sup>. The subtype *dicephalus tetrabrachius-dipus*, as observed in the present case, is considered rare (4/10,000,000 births)<sup>(5)</sup>.

US has shown to be the best method for initial evaluation of the gestation, and can identify imperfect twinning as early as at the 12th gestational week<sup>(1)</sup>. However, US is subjected to limitations such as maternal biotype and presence of either oligohydramnios

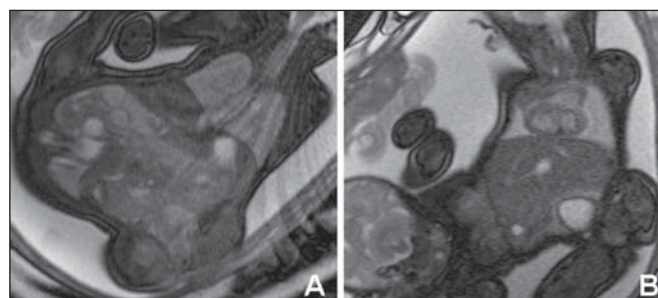


**Figure 1.** Fetal MRI T2-weighted image showing the *dicephalus tetrabrachius-dipus* conjoined twin. The fetus at right presents with a left diaphragmatic hernia. Mediastinal structures (heart and large vessels) and pulmonary hypoplasia (A) are identified. Hepatic fusion is also visualized (B).



**Figure 2.** Postnatal image of the *dicephalus tetrabrachius-dipus* twin (A). Radiographic evaluation showing vertebral spines fusion at the L4 level and a single pelvis. A diaphragmatic hernia is observed in the fetus at right (there is evidence of the presence of bowel loops within the thoracic cavity), without identification of the heart and airways (B).

or anhydramnios. On the other hand, MRI represents a good complementary tool since it does not present such limitations, while providing images with better resolution<sup>(6)</sup>. Additionally, it serves as support for a possible surgical planning, since it allows for visualization and detection of abnormalities which otherwise would be missed or inconclusive at US<sup>(2)</sup>. In the present case, MRI was relevant, particularly in the determination of the type of imperfect twinning as well as of the extent of fusion and sharing of organs.

Congenital abnormalities not related to the fusion site are observed in 10% to 20% of cases of conjoined twins. Diaphragmatic hernia such as the one observed in the present case is one of the described findings<sup>(7)</sup>. Upper eyelid coloboma that was also identified in the present case is considered to be a rare abnormality<sup>(8)</sup>.

Thus, the correct determination of the type of imperfect twinning as well as of the fusion extent may be useful in the evaluation of the condition severity and in the postnatal surgical planning. Determining the severity of the condition is of paramount importance considering that the Brazilian laws allows for gestation termination in cases where the extrauterine life is not possible<sup>(3)</sup>.

REFERENCES

1. McHugh K, Kiely EM, Spitz L. Imaging of conjoined twins. *Pediatr Radiol.* 2006;36:899–910.
2. Denardin D, Telles JA, Betat RS, et al. Imperfect twinning: a clinical and ethical dilemma. *Rev Paul Pediatr.* 2013;31:384–91.
3. Nomura RM, Brizot ML, Liao AW, et al. Conjoined twins and legal authorization for abortion. *Rev Assoc Med Bras.* 2011;57:205–10.

4. Spencer R. Theoretical and analytical embryology of conjoined twins: part I: embryogenesis. *Clin Anat.* 2000;13:36–53.
5. Martínez-Frías ML, Bermejo E, Mendioroz J, et al. Epidemiological and clinical analysis of a consecutive series of conjoined twins in Spain. *J Pediatr Surg.* 2009;44:811–20.
6. Hibbeln JF, Shors SM, Byrd SE. MRI: is there a role in obstetrics? *Clin Obstet Gynecol.* 2012;55:352–66.
7. Mackenzie TC, Crombleholme TM, Johnson MP, et al. The natural history of prenatally diagnosed conjoined twins. *J Pediatr Surg.* 2002;37:303–9.
8. Mansour AM, Mansour N, Rosenberg HS. Ocular findings in conjoined (Siamese) twins. *J Pediatr Ophthalmol Strabismus.* 1991;28:261–4.

Rafael Fabiano Machado Rosa<sup>1</sup>, Luciano Vieira Targa<sup>2</sup>, Stephan Philip Leonhardt Altmayer<sup>1</sup>, Karen Lizeth Puma Lliguin<sup>1</sup>, Daniela Denardin<sup>2</sup>, André Campos da Cunha<sup>2</sup>

1. Universidade Federal de Ciências da Saúde de Porto Alegre (UFCSPA), Porto Alegre, RS, Brasil. 2. Hospital Materno Infantil Presidente Vargas (HMIPV), Porto Alegre, RS, Brasil. Mailing Address: Dr. Rafael Fabiano Machado Rosa. Rua Sarmento Leite, 245/403, Centro. Porto Alegre, RS, Brazil, 90050-170. E-mail: rfmr@terra.com.br.

<http://dx.doi.org/10.1590/0100-3984.2013.0021>

**Epidural cavernous hemangioma of the spine: magnetic resonance imaging findings**

Dear Editor,

A previously healthy male, 52-year-old patient complaining of progressive lower limbs paraparesis for four months and recent onset of urinary incontinence, with no history of local trauma. At admission, the patient was afebrile and, at physical examination presented with spastic paraparesis with sensitive level at D8. Laboratory tests (blood count and biochemical blood tests) did not demonstrate any significant alteration.

Magnetic resonance imaging (MRI) demonstrated the presence of an elongated lesion with regular contour, intermediate signal intensity on T1-weighted and marked hypersignal on T2-weighted sequences, with intense and homogeneous contrast en-

hancement, located in the epidural space, extending from D5 to D7. Such a lesion determined a significant narrowing of the rachidian canal and medullary compression on the corresponding segments, with consequential medullary hypersignal on T2-weighted and STIR sequences compatible with compressive myelopathy (Figure 1).

The patient was submitted to surgical procedure where a wine-colored lesion compressing the dural sac was observed. The lesion was completely resected with no significant complication. Anatomopathological analysis demonstrated proliferation of middle-sized vessels filled with blood, with no atypias, compatible with cavernous hemangioma.

Hemangiomas are benign proliferative vascular lesions. According to the predominant type of vascular canal, hemangiomas are classified as follows: venous, arteriovenous, capillary and cav-



**Figure 1.** Sagittal MRI T1-weighted (A), T2-weighted (B), STIR (C) and T1-weighted sequences with fat saturation following intravenous contrast injection (D) demonstrating an elongated, expansile well-delimited lesion with regular contour, located in the epidural space of the posterior region of the dorsal spine, extending from D5 to D7. The lesion presents intermediate signal on T1-, marked hypersignal on T2-weighted and STIR sequences, with intense and homogeneous contrast enhancement, suggestive of hemangioma. Such a tumor causes remarkable narrowing of the rachidian canal, determining high signal intensity in the spinal cord (better visualized on STIR sequences) due to compressive myelopathy.